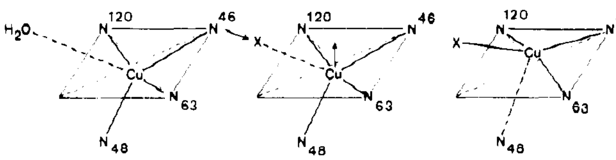

Figure 6. Scheme of the reciprocal movement of the copper ion and the X ligand: chromophore in the native enzyme (left); final arrangement in the case of a strong ligand (right).

protons to be 2×10^{-11} s.[5] The T_1 values of His-48 protons in the N_3^- derivative are consistent with a Cu–N distance of 2.7 Å, i.e. with a lengthening of about 0.6 Å. This value is sizeably higher than the value of 0.27 Å estimated from EXAFS studies,[23] but the metal to nitrogen distance is less than 20% different. A factor of 2 in the electronic relaxation time could make the two figures coincident. Note that T_1 of signal L passes from 4.3 ms in the case of the native derivative to 8.2 ms in the azide derivative. Furthermore, signal P, corresponding to Hβ1 of His-46, experiences a Cu–H distance increase of about the same amount (T_1 is 1.6 ms in the native derivative and 5.5 ms in the azide derivative). Despite that indetermination in the Cu–H distances may be relatively high, the increase in Cu–N(His-48) distance is a conceivable geometrical perturbation that may occur together with other geometrical variations. Figure 4D shows the effect of a variation of Dq of the His-48 ligand under the conditions of the right-hand side of Figure 4B, i.e., with copper being approximately in the average X, N(His-120), N(His-48), and N(His-63) plane. The effects of detaching His-48 are relatively small but in the right direction (increase of $A_\parallel$ and transition energies).

From heteronuclear NMR studies it has been suggested that F^- [12,13,52] and NCS^- [12,14] are actually bound to copper. Spectroscopic data on both Cu_2Zn_2SOD and Cu_2Co_2SOD and ligand field calculations are consistent with a small bonding interaction around the water binding position. The hyperfine shifts of His-48 are most sensitive to such binding; when no ligand is present at the water position as in the case of the Ile-137 mutant, His-48 is better bound. Azide and cyanide seem to bind quite tightly and to cause detachment of His-48 through a movement of copper. This can be schematically envisaged as in Figure 6. Cyanate has an intermediate behavior; its CD spectrum, which reveals a further transition, can be consistent with an even more distorted geometry.

Concluding Remarks. The ^{1}H NOE study of Cu_2Co_2SOD in the presence of saturating amounts of azide has shown that the interproton distances of the histidines bound to copper, and between such histidines and diamagnetic groups, are essentially the same upon azide binding. The technique of NOE in paramagnetic molecules has been pushed to its limits in order to minimize the errors. Within this frame the spectroscopic properties of the anion derivatives have been discussed on the basis of an angular overlap approach that takes into consideration the movement of copper and the binding strength and position of the anions. The $A_\parallel$ trend, $g_\parallel$ values and directions, electronic transitions in the Cu_2Zn_2 derivatives, and T_1 values of the protons of His-48 and His-46 in Cu_2Co_2SOD point to a lenghtening of the Cu–N(His-48) distance from NCS^- to CN^- ligands. This trend is consistent with the EXAFS report on the SOD anion derivatives.[23]

Registry No. L-His, 71-00-1; N_3^-, 14343-69-2; CN^-, 57-12-5; NCO^-, 661-20-1; NCS^-, 302-04-5; F^-, 16984-48-8; Cu, 7440-50-8; superoxide dismutase, 9054-89-1.

---

(52) Viglino, P.; Rigo, A.; Stevanato, R.; Ranieri, G. A.; Rotilio, G.; Calabrese, L. *J. Magn. Reson.* **1979**, *34*, 265.

Contribution from the Fujian Institute of Research on the Structure of Matter
and Fuzhou Laboratory of Structural Chemistry, Chinese Academy of Sciences, Fuzhou, Fujian 350002, China

Syntheses, Structures, and Properties of Vanadium, Cobalt, and Nickel Compounds with 2-Mercaptophenol

Beisheng Kang,* Linghong Weng, Hanqin Liu, Daxu Wu, Liangren Huang, Cenzhong Lu, Jinghua Cai, Xuetai Chen, and Jiaxi Lu

Received April 20, 1989

Three new compounds of 2-mercaptophenolate (mp^{2-}), trinuclear $(Et_4N)[V_3(mp)_6]$ (**1a**) or $(Ph_4P)[V_3(mp)_6]$ (**1b**), dimeric $(Et_4N)_2[Co(mp)(Hmp)]_2$ (**2**), and binuclear $(Et_4N)_2[Ni_2(mp)_2(Hmp)_2]$ (**3**), were synthesized and their structures determined. Compound **1b** crystallizes in the triclinic space group $P\bar{1}$ with a = 14.127 (4) Å, b = 14.342 (4) Å, c = 15.878 (4) Å, α = 65.08 (2)°, β = 73.09 (2)°, γ = 78.68 (2)°, V = 2781.3 Å^3, and Z = 2. Compound **2** crystallizes in the monoclinic space group $P2_1/c$ with a = 16.606 (2) Å, b = 15.575 (1) Å, c = 17.725 (2) Å, β = 111.07 (1)°, V = 4277.8 Å^3, and Z = 4. Compound **3** crystallizes in the monoclinic space group $P2_1/n$ with a = 9.179 (4) Å, b = 17.487 (5) Å, c = 12.840 (4) Å, β = 92.87 (3)°, V = 2058.6 Å^3, and Z = 2. Structural analyses revealed the multifunctional chelating character of mp^{2-}: it can be S_tO_t (t for terminal) as in **2**, **3**, and $(Et_4N)_2[Fe_2(mp)_4]$[13] (**4**), S_tO_b (b for bridging) as in **1b** and **4**, or S_bOH as in **3**. Some structural regularities are observed. Compounds **1b** and **2** are paramagnetic with magnetic moments of 2.76 and 2.38 μ_B per molecule in the polycrystalline state, respectively. Compound **2** dissociates in DMSO to its monomer, which is rapidly oxidized by trace air. The final product is purple $[Co(mp)_2]^-$ with a magnetic moment of 3.26 μ_B. A simulated ^{1}H NMR spectrum of **3** revealed the nuclear spin coupling of the hydrogen atom in the hydroxyl group with the ortho H on the same phenyl ring.

Introduction

Transition-metal elements are essential to many biological systems in nature. For example, the recently identified second nitrogenase[1] contains vanadium in an O_3S_3 environment.[2] The development of V chemistry has also been furthered by the desire to understand its biological role in organisms such as tunicates,[3] which contain tunichrome[4] (TC) with V(III) chelated to polypeptide chains rich in hydroxyl groups. While four- or five-coordinate Co(II) thiolates have been considered as models for the catalytic site of the cobalt-substituted alcohol dehydrogenase,[5] the V, Co, Cr, Mn, and Cu complexes of EHPG [ethylenebis-[(*o*-hydroxyphenyl)glycine]] have been studied as models for metallotransferrins.[6,7] Nickel is known to be present in the

---

* To whom correspondence should be addressed at the Fujian Institute of Research on the Structure of Matter.

(1) (a) Robson, R. L.; Eady, R. R.; Richardson, T. H.; Miller, R. W.; Hawkins, M.; Postgate, J. R. *Nature (London)* **1986**, *322*, 388. (b) Arber, J. M.; Dodson, B. R.; Eady, R. R.; Stevens, P.; Hasnain, S. S.; Garner, C. D.; Smith, B. E. *Ibid.* **1987**, *325*, 372. (c) Smith, B. E.; Eady, R. R.; Lowe, D. J.; Gormal, C. *Biochem. J.* **1988**, *250*, 299.

(2) George, G. N.; Coyle, C. L.; Hales, B. J.; Cramer, S. P. *J. Am. Chem. Soc.* **1988**, *110*, 4057.

(3) Kustin, K.; McLeod, G. C.; Gilbert, T. R.; Briggs, L. R. *Struct. Bonding (Berlin)* **1983**, *53*, 139.

(4) Oltz, E. M.; Bruening, R. C.; Smith, M. J.; Kustin, K.; Nakanishi, K. *J. Am. Chem. Soc.* **1988**, *110*, 6162.

(5) Corwin, D. J., Jr.; Fikar, R.; Koch, S. A. *Inorg. Chem.* **1987**, *26*, 3079.

0020-1669/90/1329-4873$02.50/0

hydrogenases from several types of bacteria[8] including the sulfate-reducing bacterium *Desulfovibrio gigas*. A study of these enzymes indicates the presence of M–S and/or M–O bonds essential to their biological activities.

Studies on metal compounds with either thiolato or phenolato ligands have been abundantly reported for simulation of either the active-site structures or redox properties of metalloenzymes, but those on compounds containing ligand atoms O and S simultaneously at 1,2-positions are scarce.[9] In our extensive study of the coordination chemistry of transition-metal compounds with 2-mercaptophenol (H_2mp), three new compounds, trinuclear $(Ph_4P)[V_3(mp)_6]$ (**1b**), dimeric $(Et_4N)_2[Co(mp)(Hmp)]_2$[10] (**2**), and binuclear $(Et_4N)_2[Ni_2(mp)_2(Hmp)_2]$[11] (**3**), have been synthesized following the investigation on the 5-coordinate diiron-sulfur compound $(Et_4N)_2[Fe_2(mp)_4]$[12,13] (**4**). The syntheses, structures, and properties of **1**–**3** are reported in this paper.

Experimental Section

All operations were carried out under a dinitrogen atmosphere with Schlenk techniques. Reagents VCl_3 (Aldrich), $CoCl_2{\cdot}6H_2O$, (Tianjin), $NiCl_2{\cdot}6H_2O$ (Shanghai), and 2-mercaptophenol (Merck-Schuchardt) were used as obtained commercially. Solvents were dried over molecular sieves and distilled under dinitrogen before use (EtOH over $Mg(OEt)_2$, MeCN over P_2O_5, DMF over CaH_2). Precipitation agents Ph_4PBr and Et_4NX (X = Cl, Br) were used as obtained. Sodium methoxide was synthesized by dissolving sodium metal in dry methanol and dried under reduced pressure. Elemental analyses were performed by the chemical analysis group of this institute.

Preparation of Compounds. $(Et_4N)[V_3(mp)_6]$ (1a). To a solution of 0.324 g (1.90 mmol) of Na_2mp (obtained from 0.197 mL of H_2mp (d = 1.22 g/cm^3, 1.91 mmol) and 0.206 g (3.81 mmol) of NaOMe) in 10 mL of absolute EtOH was added 0.15 g (0.95 mmol) of VCl_3 in 15 mL of absolute EtOH. After the mixture was stirred at room temperature for 30 min and filtered, the purple filtrate was combined with precipitation agent.

When Et_4NCl (0.158 g, 0.95 mmol) in 10 mL of EtOH was added, the above solution gave dark purple microcrystals of **1a** (30% yield) on standing at 5 °C for 10 days. IR (KBr; cm^{-1}): 3030 (w), 2960 (w), 1550 (w), 1440 (s), 1430 (s), 1380 (w), 1285 (w), 1255 (s), 1228 (m), 860 (m, br), 750 (s), 690 (m), 600 (m, br), 414 (m), 380 (m). ^1H NMR (CD_3CN; δ, ppm): 4.95 (br), 9.30 (br).

$(Ph_4P)[V_3(mp)_6]$ (1b). Due to the poor quality of crystalline **1a** for X-ray analysis, compound **1b** was synthesized by the same procedures except that the purple solution was combined with 0.40 g (0.95 mmol) of Ph_4PBr in 15 mL of EtOH to give a dark purple solid, which was collected, washed with EtOH, and dried in vacuo to give approximately 0.2 g of crude product (50% based on vanadium) contaminated with inorganic salt (NaCl). On repeated recrystallization from MeCN at 60 °C and the last crystallization maintained at ambient temperature for 3 weeks, well-shaped purple pillar crystals of compound **1b** were formed that showed essentially the same IR absorptions as those for **1a** except for those of the cations; yield 10%. IR (KBr; cm^{-1}): 3040 (w), 1555 (w), 1480 (w), 1450 (s), 1430 (s), 1290 (w), 1255 (s), 1222 (s), 1102 (s), 860 (s, br), 750 (sh), 740 (s), 720 (s), 685 (s), 600 (s, br), 520 (s), 415 (s), 385 (s). The compound was scarcely soluble in CD_3CN or DMSO.

Table I. Data Collection and Crystallographic Parameters

	1b	**2**	**3**
formula	$C_{60}H_{44}O_6PS_6V_3$	$C_{40}H_{58}Co_2N_2O_4S_4$	$C_{40}H_{58}N_2Ni_2O_4S_4$
fw	1237.3	877.04	876.60
crystal system	triclinic	monoclinic	monoclinic
space group	$P\bar{1}$	$P2_1/c$	$P2_1/n$
a, Å	14.127 (4)	16.606 (2)	9.179 (4)
b, Å	14.342 (4)	15.575 (1)	17.487 (5)
c, Å	15.878 (4)	17.725 (2)	12.840 (4)
α, deg	65.08 (2)		
β, deg	73.09 (2)	111.07 (1)	92.87 (3)
γ, deg	78.68 (2)		
V, Å^3	2781.3	4277.8	2058.6
Z	2	4	2
d_c, g/cm^3	1.48	1.36	1.41
μ, cm^{-1}	7.7	10.2	11.5
diffractometer	CAD-4	AFC-5R	CAD-4
scan range, deg	$2 < 2\theta < 50$	$2 < 2\theta < 50$	$2 < 2\theta < 46$
no. of unique reflcns ($I > 3\sigma(I)$)	5733	3544	1646
no. of params refined	688	435	235
no. of $F(000)$ values	1264	2264	928
R	0.063	0.064	0.076
R_w	0.065	0.066	0.079

$(Et_4N)_2[Co(mp)(Hmp)]_2$ (2). A solution of 0.20 g (0.84 mmol) of $CoCl_2{\cdot}6H_2O$ in 10 mL of MeCN was added to a mixture of 0.182 g (3.37 mmol) of NaOMe and 0.212 g (1.68 mmol) of H_2mp in 10 mL of MeCN to give a dark green solution. After the mixture was stirred for 30 min at room temperature, an EtOH solution of 0.353 g (1.68 mmol) of Et_4NBr was added. After filtration, 0.2 g of dark red pillar crystals of **2** (yield 54%) was obtained from the filtrate on standing at 5 °C for 1 week. IR (paraffin oil; cm^{-1}): 3020 (w), 2970 (w), 2542 (w), 1555 (s), 830 (s), 775 (m), 745 (s), 725 (m), 675 (m), 600 (m, br), 565 (m), 410 (m), 375 (m), 265 (s). Anal. Calcd for $C_{40}H_{58}Co_2N_2O_4S_4$: Co, 13.44; N, 3.19; S, 14.62. Found: Co, 13.48; N, 3.94; S, 14.02.

A solution of **2** in DMSO-d_6 was easily oxidized by air, and the final product showed ^1H NMR signals at δ −14.3 (d), −16.2 (d), −27.3 (t), and −31.7 (t) ppm.

$(Et_4N)_2[Ni_2(mp)_2(Hmp)_2]$ (3). To a solution of 2.1 g (12.3 mmol) of Na_2mp in 20 mL of absolute EtOH was added a solution of 0.98 g (4.11 mmol) of $NiCl_2{\cdot}6H_2O$ in 15 mL of EtOH within 15 min, during which period the reaction solution changed color from light yellow through reddish brown to brownish green. After continuous stirring for 30 min until the color no longer changed, the solution was filtered and combined with 0.61 g (2.88 mmol) of Et_4NBr in 15 mL of EtOH. A brown precipitate formed immediately, and the solution was kept at 5 °C for a few hours and filtered. The crude product was recrystallized from DMF/MeCN (1:2) and gave 0.9 g of dark brown needle crystals of **3** (yield 50%). IR (KBr; cm^{-1}): 3040 (w), 2980 (w), 2550 (w), 1550 (m), 840 (m), 780 (m), 765 (s), 745 (s), 725 (m), 682 (m), 665 (w), 640 (w), 575 (w), 450 (m), 400 (w), 375 (w), 330 (w), 300 (w). ^1H NMR (DMSO-d_6; δ, ppm): 6–7 (m), 9.6 (d). Anal. Calcd for $C_{40}H_{58}N_2Ni_2O_4S_4$: H, 6.67; Ni, 13.39; N, 3.20. Found: H, 6.16; Ni, 12.88; N, 4.00.

Structure Determination. Single crystals of compounds **1b**, **2**, and **3** of suitable dimensions were sealed inside glass capillaries under dinitrogen. Diffraction data were collected on four-circle diffractometers in the ω–2θ scan mode with Mo Kα radiation (λ = 0.71073 Å) and a graphite monochromator. The parameters utilized in intensity collections and refinements are summarized in Table I together with the crystallographic data. All calculations were performed on a VAX-11/785 computer using the SDP/VAX program package.

The intensity data collected were corrected for Lp factors and empirical absorptions. The structures of **1b** and **2** were solved by direct methods; that of **3** was solved by the heavy-atom method. All the final structures were determined by difference Fourier syntheses and refined by full-matrix least-squares techniques with anisotropic thermal parameters for all the non-hydrogen atoms. Selected bond lengths and bond angles are collected in Tables II–IV.

Physical Measurements. Infrared spectra were recorded on a Perkin-Elmer 577 spectrophotometer. ^1H NMR spectra were obtained on a Varian FT-80A spectrometer with TMS as the internal standard. Magnetic susceptibilities for the solid state were measured on a Gouy-Faraday magnetic balance with the Faraday method,[14] and those in solution were obtained by the ^1H NMR method.[15]

Results and Discussions

The reactions of metal chlorides with 2-mercaptophenol have not been very much explored, except for an early study of elec-

---

(6) Patch, M. G.; Simolo, K. P.; Carrano, C. J. *Inorg. Chem.* **1982**, *21*, 2972.

(7) Bonadies, J. A.; Carrano, C. J. *J. Am. Chem. Soc.* **1986**, *108*, 4088.

(8) Thomson, A. J. *Nature (London)* **1982**, *298*, 602.

(9) Balch, A. L. *J. Am. Chem. Soc.* **1969**, *91*, 1948.

(10) Preliminary structural data have been communicated: Weng, L. H.; Huang, L. R.; Kang, B. S. *Jiegou Huaxue* **1989**, *8*, 136. The structural parameters have since been refined.

(11) Lu, C. Z.; Cai, J. H.; Huang, Z. Y.; Weng, L. H.; Kang, B. S. *Jiegou Huaxue* **1988**, *7*, 241.

(12) Kang, B. S.; Weng, L. H.; Wu, D. X.; Wang, F.; Guo, Z.; Huang, L. R.; Huang, Z. Y.; Liu, H. Q. *Inorg. Chem.* **1988**, *27*, 1128.

(13) Kang, B. S.; Weng, L. H.; Wu, D. X.; Huang, L. R.; Wang, F.; Guo, Z.; Liu, H. Q. *Inorg. Chim. Acta* **1988**, *148*, 147.

(14) Liu, H. Q.; Liu, Q. T.; Kang, B. S.; He, L. J.; Chen, C. N.; Zhao, K.; Hong, M. C.; Huang, L. R.; Zhuang, J.; Lu, J. X. *Sci. Sin., Ser. B (Engl. Ed.)* **1988**, *31*, 10.

(15) Evans, D. F.; James, T. A. *J. Chem. Soc., Dalton Trans.* **1979**, 723.

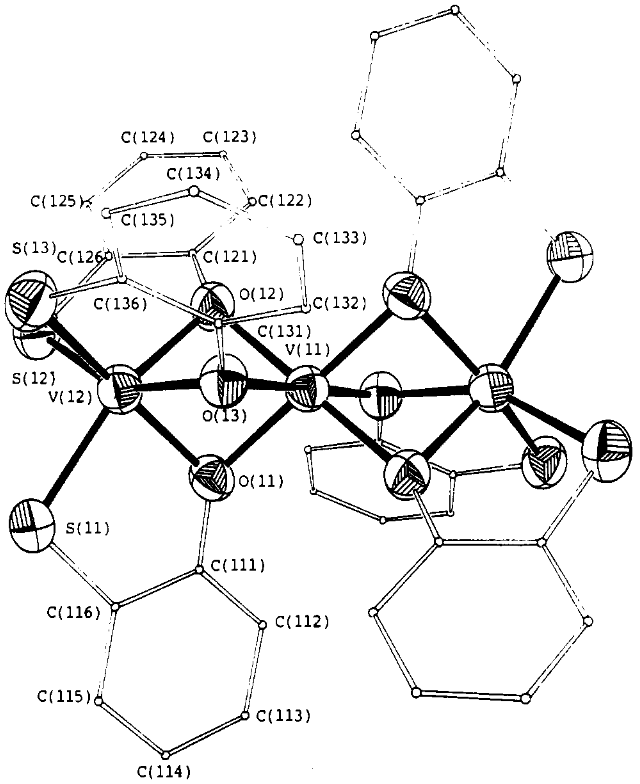

Figure 1. Structure of the anion $[V_3(mp)_6]^-$. Carbon atoms are represented by spheres of arbitrary size for clarity.

tron-transfer and magnetic properties of mononuclear Co, Ni, Cu, and Zn compounds, which were obtained from 50% aqueous ethanol.[9] When $MCl_x \cdot yH_2O$ (M = V, $x = 3$, $y = 0$; M = Co, Ni, $x = 2$, $y = 6$) was reacted with Na_2mp in anhydrous protic solvent ethanol or aprotic solvent acetonitrile, a trinuclear or dinuclear compound was obtained. It has been observed that the mp^{2-}:MCl_x ratio is important in obtaining an individual compound. Compound **1** was isolated from the reaction with a 2:1 mp^{2-}:VCl_3 mixture. If 3 equiv of mp^{2-} was employed in the reaction process, a different crystalline product of formula $(Ph_4P)_2[NaV(mp)_3(MeCN)(MeOH)]_2$[16] (**5**) was isolated.

Compound **3** was prepared from a mp^{2-}:$NiCl_2$ ratio of 3:1. If the amount of mp^{2-} is decreased to 2 equiv, a very air-sensitive crystalline product[17] can be isolated, which awaits further investigation. Hydroxyl groups are present in compounds **2** and **3**, as inferred by electronic charge balance. Strong intramolecular hydrogen bonding may result in the absence of characteristic hydroxyl absorptions in the IR spectra.

The compounds are all composed of discrete cations and anions, and the former as Et_4N^+ and Ph_4P^+ salts have normal structures and will not be discussed here. The anionic structures of **1b**, **2**, and **3** are shown in Figures 1–3, respectively.

Compound 1b. There are two anions of compound **1b** in one unit cell centered at (0, 0, 0) and ($^1/_2$, $^1/_2$, $^1/_2$), while the two discrete Ph_4P^+ cations are located closely at ($^1/_4$, $^1/_4$, $^1/_4$) and ($^3/_4$, $^3/_4$, $^3/_4$). Figure 4 shows the packing of molecules in half of a unit cell for clarity.

The three V atoms in an anion are arranged in a linear fashion (V(n2)-V(n1)-V(n2') = 180.0°, n = 1 or 2), forming the pseudo-C_3 axis. Two independent anions, each of which possesses pseudo-S_6 symmetry with the inversion center on the central atom V(n1), are nearly perpendicular to each other (80.1°). Three mp^{2-} ligands provide three terminal thiolates for V(n2) and three μ_2-aryloxy bridges to connect atoms V(n1) and V(n2). Selected atomic distances and bond angles of the anion of **1b** are listed in Table II. The V atoms are all six-coordinated: atom V(n1) in the center of a severely distorted octahedron (average O(nm)-V(n1)-O(nm') ≅ 80°, m, m' = 1, 2, 3; $m \neq m'$) of six oxygen

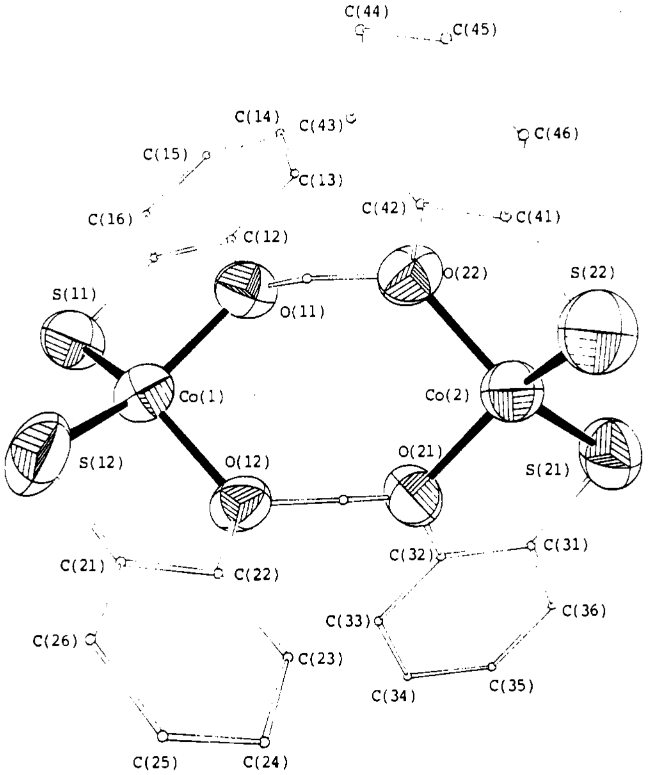

Figure 2. Structure of the anion $[Co(mp)(Hmp)]_2^{2-}$. Carbon atoms are represented by spheres of arbitrary size for clarity.

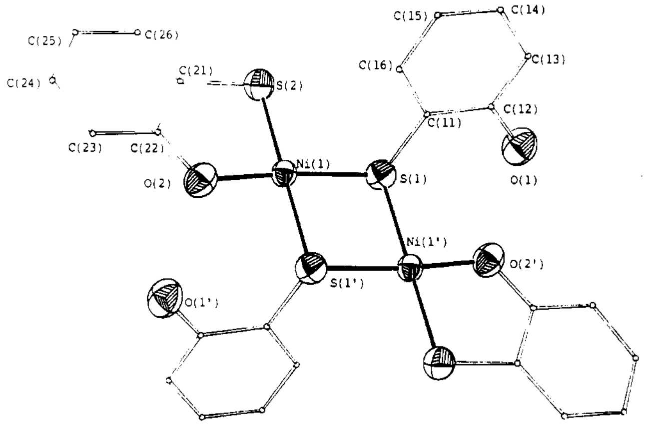

Figure 3. Structure of the anion $[Ni_2(mp)_2(Hmp)_2]^{2-}$. Carbon atoms are represented by spheres of arbitrary size for clarity.

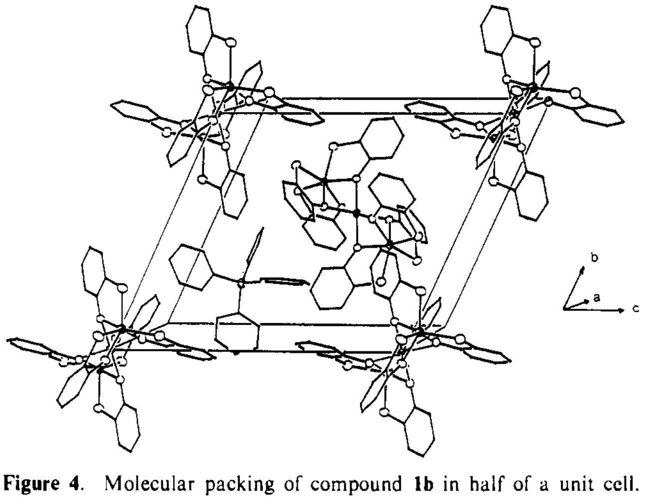

Figure 4. Molecular packing of compound **1b** in half of a unit cell.

---

(16) During the review of this paper, the crystal structure of **5** has been determined and will be published elsewhere.

(17) Lu, C. Z. Unpublished result.

Table II. Selected Atomic Distances (Å) and Bond Angles (deg) for the Anion $[V_3(mp)_6]^-$

Distances			
V(11)–V(12)	2.7205 (9)	V(21)–V(22)	2.720 (1)
V(11)–O(11)	1.982 (4)	V(21)–O(21)	1.985 (3)
V(11)–O(12)	1.964 (3)	V(21)–O(22)	1.932 (3)
V(11)–O(13)	1.973 (3)	V(21)–O(23)	1.984 (3)
V(12)–S(11)	2.290 (2)	V(22)–S(21)	2.300 (2)
V(12)–S(12)	2.283 (2)	V(22)–S(22)	2.288 (2)
V(12)–S(13)	2.307 (2)	V(22)–S(23)	2.304 (2)
V(12)–O(11)	2.001 (3)	V(22)–O(21)	1.994 (3)
V(12)–O(12)	2.017 (3)	V(22)–O(22)	2.009 (3)
V(12)–O(13)	2.025 (3)	V(22)–O(23)	2.007 (3)
Angles			
V(12)–V(11)–V(12′)	180.01 (2)	V(22)–V(21)–V(22′)	180.01 (2)
O(11)–V(11)–O(12)	79.1 (1)	O(21)–V(21)–O(22)	79.5 (1)
O(11)–V(11)–O(13)	79.9 (1)	O(21)–V(21)–O(23)	77.9 (1)
O(12)–V(11)–O(13)	79.7 (1)	O(22)–V(21)–O(23)	79.8 (1)
O(11)–V(11)–O(11′)	180.01 (2)	O(21)–V(21)–O(21′)	180.01 (2)
O(12)–V(11)–O(12′)	180.01 (1)	O(22)–V(21)–O(22′)	180.01 (1)
O(13)–V(11)–O(13′)	180.01 (1)	O(23)–V(21)–O(23′)	180.01 (1)
O(11)–V(11)–O(12′)	100.9 (1)	O(21)–V(21)–O(22′)	100.5 (1)
V(11)–O(11)–V(12)	86.2 (1)	V(21)–O(21)–V(22)	86.2 (1)
V(11)–O(12)–V(12)	86.3 (1)	V(21)–O(22)–V(22)	87.2 (1)
V(11)–O(13)–V(12)	85.8 (1)	V(21)–O(23)–V(22)	85.9 (1)
S(11)–V(12)–S(12)	94.13 (6)	S(21)–V(22)–S(22)	93.19 (6)
S(11)–V(12)–S(13)	94.68 (6)	S(21)–V(22)–S(23)	93.61 (6)
S(12)–V(12)–S(13)	91.87 (6)	S(22)–V(22)–S(23)	92.26 (7)
S(11)–V(12)–O(11)	81.8 (1)	S(21)–V(22)–O(21)	81.5 (2)
S(11)–V(12)–O(12)	155.3 (1)	S(21)–V(22)–O(22)	154.1 (1)
S(11)–V(12)–O(13)	111.6 (2)	S(21)–V(22)–O(23)	112.4 (2)
S(12)–V(12)–O(11)	112.2 (2)	S(22)–V(22)–O(21)	113.5 (1)
S(12)–V(12)–O(12)	81.6 (2)	S(22)–V(22)–O(22)	81.6 (2)
S(12)–V(12)–O(13)	153.6 (2)	S(22)–V(22)–O(23)	153.8 (1)
S(13)–V(12)–O(11)	155.8 (2)	S(23)–V(22)–O(21)	153.9 (1)
S(13)–V(12)–O(12)	109.8 (2)	S(23)–V(22)–O(22)	112.0 (1)
S(13)–V(12)–O(13)	81.0 (1)	S(23)–V(22)–O(23)	81.2 (2)
O(11)–V(12)–O(12)	77.4 (1)	O(21)–V(22)–O(22)	77.5 (1)
O(11)–V(12)–O(13)	78.2 (1)	O(21)–V(22)–O(23)	77.2 (1)
O(12)–V(12)–O(13)	77.1 (1)	O(22)–V(22)–O(23)	77.5 (1)
V(12)–S(11)–C(116)	100.5 (2)	V(22)–S(21)–C(216)	100.9 (2)
V(12)–S(12)–C(126)	100.4 (2)	V(22)–S(22)–C(226)	100.1 (2)
V(12)–S(13)–C(136)	101.0 (2)	V(22)–S(23)–C(236)	100.7 (2)
V(11)–O(11)–C(111)	138.8 (4)	V(21)–O(21)–C(211)	138.9 (4)
V(12)–O(11)–C(111)	123.7 (3)	V(22)–O(21)–C(211)	124.4 (3)
V(11)–O(12)–C(121)	145.0 (3)	V(21)–O(22)–C(221)	142.7 (3)
V(12)–O(12)–C(121)	123.7 (3)	V(22)–O(22)–C(221)	123.6 (3)
V(11)–O(13)–C(131)	136.4 (4)	V(21)–O(23)–C(231)	139.6 (3)
V(12)–O(13)–C(131)	123.5 (4)	V(22)–O(23)–C(231)	123.8 (3)

atoms (O_6) elongated along the pseudo-C_3 axis and atom V(*n*2) in a distorted trigonal prism (O_3S_3) with a twist angle of about 30° between planes O_3 and S_3.

It is interesting to note that the V–S distance of 2.30 ± 0.01 Å (mean value and standard deviation) is the shortest known for vanadium thiolates with 1,2-bidentate ligands.[18-20] The V–O bonds are of two distinct types with bonds V(*n*2)–O(*nm*) slightly but noticeably longer than bonds V(*n*1)–O(*nm*), being 2.01 ± 0.01 and 1.97 ± 0.02 Å, respectively. While V(*n*2)–O(*nm*) bonds are comparable to V–O bonds in $[V(OPh)_6]^{3-}$[21] (2.015 Å) and $[V(cat)_3]^{3-}$[22] (2.013 Å), the V(*n*1)–O(*nm*) bonds are comparable to that in [VO(HSHED)(ACAC)][23] (1.972 Å).

Considering the total apparent oxidation states (11+) and the symmetry arrangement, it is likely that the valence states of the vanadium atoms are V(*n*2)(IV)–V(*n*1)(III)–V(*n*2′)(IV). The measured magnetic moment of polycrystalline **1b** at 285 K is 2.76 μ_B. A preliminary ^1H NMR study also revealed the paramagnetic nature of **1** (see Experimental Section).

Table III. Selected Bond Distances (Å) and Bond Angles (deg) for the Anion $[Co(mp)(Hmp)]_2^{2-}$

Distances			
Co(1)–S(11)	2.252 (2)	S(22)–C(41)	1.753 (6)
Co(1)–S(12)	2.250 (2)	O(11)–O(22)	2.415 (5)
Co(1)–O(11)	2.009 (4)	O(11)–C(12)	1.355 (6)
Co(1)–O(12)	1.993 (3)	O(11)–H(1)	1.001 (3)
Co(2)–S(21)	2.266 (2)	O(12)–O(21)	2.419 (5)
Co(2)–S(22)	2.254 (2)	O(12)–C(22)	1.359 (6)
Co(2)–O(21)	1.991 (4)	O(12)–H(11)	1.419 (3)
Co(2)–O(22)	2.008 (3)	O(21)–C(32)	1.356 (6)
S(11)–C(11)	1.755 (6)	O(21)–H(11)	1.001 (3)
S(12)–C(21)	1.744 (6)	O(22)–C(42)	1.369 (6)
S(21)–C(31)	1.752 (6)	O(22)–H(1)	1.432 (3)
Angles			
S(11)–Co(1)–S(12)	115.46 (7)	O(22)–O(11)–C(12)	118.6 (3)
S(11)–Co(1)–O(11)	86.4 (2)	Co(1)–O(12)–O(21)	122.9 (2)
S(11)–Co(1)–O(12)	139.6 (1)	Co(1)–O(12)–C(22)	118.2 (3)
S(12)–Co(1)–O(11)	141.6 (1)	O(21)–O(12)–C(22)	115.4 (4)
S(12)–Co(1)–O(12)	86.7 (2)	Co(2)–O(21)–O(12)	121.2 (3)
O(11)–Co(1)–O(12)	96.2 (1)	Co(2)–O(21)–C(32)	118.6 (3)
S(21)–Co(2)–S(22)	117.36 (7)	O(12)–O(21)–C(32)	120.7 (5)
S(21)–Co(2)–O(21)	86.3 (2)	Co(2)–O(22)–O(11)	122.5 (3)
S(21)–Co(2)–O(22)	139.5 (1)	Co(2)–O(22)–C(42)	116.7 (3)
S(22)–Co(2)–O(21)	137.5 (1)	O(11)–O(22)–C(42)	114.4 (5)
S(22)–Co(2)–O(22)	87.0 (2)	S(11)–C(11)–C(12)	120.6 (4)
O(21)–Co(2)–O(22)	96.7 (1)	O(11)–C(12)–C(11)	117.9 (5)
Co(1)–S(11)–C(11)	96.5 (2)	S(12)–C(21)–C(22)	120.0 (4)
Co(1)–S(12)–C(21)	96.7 (2)	O(12)–C(22)–C(21)	118.4 (5)
Co(2)–S(21)–C(31)	96.1 (2)	S(21)–C(31)–C(32)	120.8 (4)
Co(2)–S(22)–C(41)	96.7 (3)	O(21)–C(32)–C(31)	118.0 (5)
Co(1)–O(11)–O(22)	123.0 (2)	S(22)–C(41)–C(42)	119.8 (5)
Co(1)–O(11)–C(12)	118.5 (3)	O(22)–C(42)–C(41)	119.8 (6)

Table IV. Selected Bond Distances (Å) and Bond Angles (deg) for the Anion $[Ni_2(mp)_2(Hmp)_2p^{2-}$

Distances			
Ni(1)–S(1)	2.190 (2)	S(1)–C(11)	1.768 (9)
Ni(1)–S(2)	2.160 (3)	S(2)–C(21)	1.741 (9)
Ni(1)–O(2)	1.852 (4)	O(1)–C(12)	1.334 (8)
Ni(1)–S(1′)	2.216 (3)	O(2)–C(22)	1.367 (9)
Angles			
S(1)–Ni(1)–S(2)	95.0 (1)	Ni(1)–S(1)–Ni(1′)	95.3 (1)
S(1)–Ni(1)–O(2)	174.6 (2)	C(11)–S(1)–Ni(1′)	106.2 (3)
S(1)–Ni(1)–S(1′)	84.8 (1)	Ni(1)–O(2)–C(22)	117.9 (5)
S(2)–Ni(1)–O(2)	90.5 (2)	Ni(1)–S(1)–C(11)	108.5 (4)
S(2)–Ni(1)–S(1′)	179.5 (1)	Ni(1)–S(2)–C(21)	96.8 (4)
O(2)–Ni(1)–S(1′)	89.8 (2)		

Compound 2. The selected bond distances and bond angles in the anion of **2** are shown in Table III. The anion is a dimer with two $[Co(mp)(Hmp)]^-$ fragments connected by two strong hydrogen bonds through atoms O(11)···O(22) and O(12)···O(21) with an average atomic distance of 2.416 ± 0.002 Å. Due to geometrical restriction of the five-membered ring $\overline{\text{C–O–Co–S–C}}$ (average internal angle S–Co–O = 86.6°) and the limitation of hydrogen bonds (average O–Co–O = 96.4°), the tetrahedral coordination of Co(II) is severely distorted with the angle S–Co–S of 116.4°. Tetrahedral coordination has been observed for Co(II)–S complexes with symmetrical substituents such as in $[Co(edt)_2]^{2-}$.[24] The Co–S distance of 2.256 Å is comparable to the terminal Co–S distances in $[Co_4(SPh)_{10}]^{2-}$[25] (2.258 Å) and slightly shorter than that in the alkanethiolato analogue $[Co_4(SC_2H_4OH)_{10}]^{2-}$[26] (2.269 Å).

The magnetic moment of polycrystalline **2** at 289.5 K is 2.38 μ_B per dimer. When **2** is dissolved in DMSO, it dissociates into the green monomer, which turns immediately to purple on allowing air to enter the NMR tube and the measured magnetic moment

---

(18) Money, J. K.; Nicholson, J. R.; Huffman, J. C.; Christou, G. *Inorg. Chem.* **1986**, *25*, 4072.

(19) Money, J. K.; Huffman, J. C.; Christou, G. *Inorg. Chem.* **1988**, *27*, 507.

(20) Money, J. K.; Huffman, J. C.; Christou, G. *Inorg. Chem.* **1985**, *24*, 3297.

(21) Wilisch, W. C. A.; Scott, M. J.; Armstrong, W. H. *Inorg. Chem.* **1988**, *27*, 4333.

(22) Cooper, S. R.; Koh, Y. B.; Raymond, K. N. *J. Am. Chem. Soc.* **1982**, *104*, 5092.

(23) Li, X. H.; Lah, M. S.; Pecoraro, V. L. *Inorg. Chem.* **1988**, *27*, 4657. H_2SHED = *N*-salicylidene-*N*′-(2-hydroxyethyl)ethylenediamine.

(24) (a) Pulla Rao, Ch.; Dorfman, J. R.; Holm, R. H. *Inorg. Chem.* **1986**, *25*, 428. (b) Mukherjee, R. N.; Pulla Rao, Ch.; Holm, R. H. *Inorg. Chem.* **1986**, *25*, 2979. edt = ethanedithiolate.

(25) Dance, I. G.; Calabrese, J. C. *J. Chem. Soc., Chem. Commun.* **1975**, 762; *J. Am. Chem. Soc.* **1979**, *101*, 6264.

(26) Kang, B. S.; Cai, J. H. *Jiegou Huaxue* **1988**, *7*, 199.

Table V. Comparison of Relevant Atomic Distances (Å) and Bond Angles (deg) in a C–O–M–S–C Chelate Ring

	atomic dist, Å		bond angle, deg		
compd	O–S	M–M	O–M–S	M–O–C	M–S–C
$(Ph_4P)[V_3(mp)_6]$	2.82	2.721	81.4	123.6	100.6
$(Et_4N)_2[Fe_2(mp)_4]^a$	2.93	3.165	88.2 (t)^b 83.6 (b)^b	120.7	94.8
$(Et_4N)_2[Co(mp)(Hmp)]_2$	2.94	4.896	86.7	118.0	96.5
$(Et_4N)_2[Ni_2(mp)_2(Hmp)_2]$	2.86	3.255	90.5	117.9	96.8

[a] From refs 12 and 13. [b] t for terminal and b for bridge.

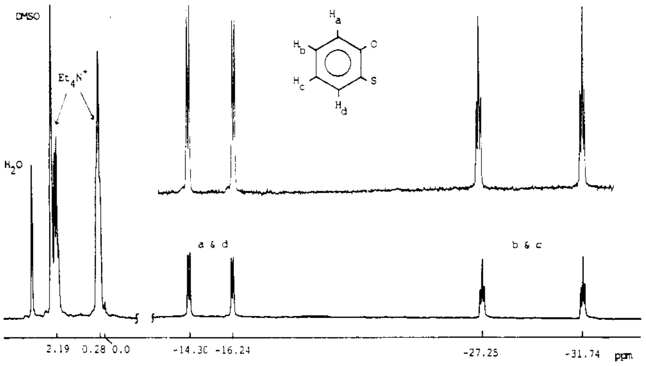

Figure 5. ^1H NMR spectrum of a solution of $(Et_4N)_2[Co(mp)(Hmp)]_2$ in DMSO-d_6 in the presence of trace air and with TMS internal standard at ambient temperature.

decreases. In the meantime, the width of the resonance absorptions decreases gradually and fine structures appear. The final product gives very sharp and well-defined ^1H NMR absorptions at high field from TMS, as shown in Figure 5. The α-H signals from the O(H_a) and S(H_d) chelate atoms of mp^{2-} appeared at −14.30 and −16.24 ppm as two doublets, while the two β-H (H_b and H_c) signals appeared at −27.25 and −31.74 ppm as two triplets. The magnetic moment meausured by the ^1H NMR technique is 3.3 ± 0.1 μ_B, similar to the literature value of 3.2 μ_B for the purple compound $(Bu_4N)[Co(mp)_2]$, which was also synthesized from the Co(II) compound by contact with a stream of air.[9]

Compound 3. Selected bond distances and bond angles of the centrosymmetric anion of compound **3** are listed in Table IV. The atoms S(1), S(1′), Ni(1), Ni(1′), O(1), O(2), S(1), and S(2) are coplanar and form the molecular plane. The terminal phenyl rings are essentially in the molecular plane, while the planes of the phenyl rings of the bridging ligands are tilted 112.9° from it. The nickel atom is at the center of the nearly square-planar environment of OS_3. Nickel compounds containing Ni–O bonds in square-planar arrangements are relatively few.[27,28] The Ni–O(2) distance of 1.852 Å is slightly shorter than the Ni–O bond in $(Ph_4P)_2[Ni_3(SCH(CH_3)COO)_4]$[28] (1.875 Å), probably due to the terminal chelating nature of the mp^{2-} ligand. The Ni(1)–S(1) bond being longer than the Ni(1)–S(2) bond by 0.03 Å agrees with the observation of Nicholson[29] that the M–S bond inside a five-membered chelate ring is shorter than that outside, which is also true for compound **4**.[12,13] The free hydroxyl group on the bridge ligand is near the atom O(2) of the terminal mp^{2-} (O(1)···O(2′) 2.539 Å), and strong hydrogen bonding is obvious. The hydrogen bond and the diamagnetic nature of compound **3** in DMSO solution are revealed by ^1H NMR results.[30]

All the compounds containing mercaptophenolate ligands have five-membered chelate rings C–S–M–O–C similar to those of the extensively studied dithiolenes,[31] with two sulfur donor atoms. The bite angles O–M–S and the bite distances O–S are compared in Table V together with relevant bond angles. The bite angles of mp^{2-} span a range of 9°, while the bite distances average 2.89 Å, with a maximum deviation of only 0.07 Å. The V compound **1b** has the shortest bite distances and the smallest bite angles due to the bridging nature of the mp^{2-} ligand. The congestion of the six-coordinate environment of the V atoms with triple bridges may also cause the slight decrease in the expanse of the O–M–S angles. A smaller bite angle for the bridging ligand than for the terminal chelate ligand was also observed for **4**.[12,13] The M–O–C angles of ~120° are much larger than the M–S–C angles of ~97° due to the different orbitals for bonding of the O and S atoms. The oxygen donor atom is sp^2 hybridized, while the bonding orbitals of the sulfur donor atom are mainly of p character.

These results show that 2-mercaptophenol is a multifunctional ligand in its chelation to transition-metal atoms, whether terminal S_tO_t as in compounds **2–4**, oxo-bridging S_tO_b as in **1b** and **4**, or sulfido-bridging S_bOH as in **3**:

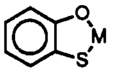

S_tO_t

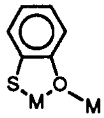

S_bO_b

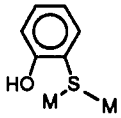

S_bOH

Acknowledgment. This work was supported by grants from the NNSF and SFCAS. The experimental assistance of Cai Suhua, Chen Bo, Wu Qiangjin, and Lin Housong and stimulating discussions with Huang Zhiying are greatly appreciated.

Registry No. **1a**, 129916-75-2; **1b**, 129916-76-3; **2**, 126183-94-6; **3**, 119127-36-5; $[Co(mp)_2]^-$, 46761-60-8.

Supplementary Material Available: Listings of positional and thermal parameters, refined displacement parameters (U's), complete bond distances and angles, and least-squares planes for anions of compounds **1b**, **2**, and **3** (18 pages). Ordering information is given on any current masthead page.

---

(27) (a) Bond, A. M.; Haga, M.; Creece, I. S.; Robson, R.; Wilson, J. C. *Inorg. Chem.* **1988**, *27*, 712. (b) Ray, D.; Pal, S.; Chakravoty, A. *Inorg. Chem.* **1986**, *25*, 2676.

(28) Rosenfield, S. G.; Wong, M. L.; Stephan, D. W.; Mascharak, P. K. *Inorg. Chem.* **1987**, *26*, 4119.

(29) Nicholson, J. R.; Christou, G.; Huffman, J. C.; Folting, K. *Polyhedron* **1987**, *6*, 863.

(30) Liu, H. Q.; Wu, D. X.; Chen, X. T.; Kang, B. S. *Chin. J. Magn. Reson.* **1990**, *7*, 231.

(31) Examples: Eisenberg, R. *Prog. Inorg. Chem.* **1970**, *12*, 295, and references cited therein. Balch, A. L.; Dance, I. G.; Holm, R. H. *J. Am. Chem. Soc.* **1968**, *90*, 1139. Balch, A. L. *J. Am. Chem. Soc.* **1969**, *91*, 6962. Vance, C. T.; Bereman, R. D.; Bordner, J.; Hatfield, W. E.; Helms, J. H. *Inorg. Chem.* **1985**, *24*, 2905.